International Journal of the Physical Sciences Vol. 7(2), pp. 191 - 204, 9 January, 2012
Available online at http://www.academicjournals.org/IJPS
DOI: 10.5897/IJPS11.1476
ISSN 1992-1950 ©2012 Academic Journals

Full Length Research Paper

Effects of induced magnetic field and slip condition on peristaltic transport with heat and mass transfer in a non-uniform channel

Najma Saleem[1], T. Hayat[2]* and A. Alsaedi[3]

[1]Department of Mathematics, University of Management and Technology, CII Johar Town Lahore-54770, Pakistan.
[2]Department of Mathematics, Quaid-i-Azam University Islamabad 44000, Pakistan.
[3]Department of Mathematics, Faculty of Science, King Abdulaziz University, P. O. Box 80257, Jeddah 21589, Saudi Arabia.

Accepted 12 October, 2011

We study the effects of induced magnetic field and slip on the peristaltic flow of Jeffrey fluid in a non-uniform channel. Flow analysis is discussed in the presence of heat and mass transfer. Main emphasis is given to the study of stream function, the longitudinal pressure gradient, the magnetic force function, the axial induced magnetic field, the current density, the temperature and concentration. Numerical integration is carried out for pressure rise per wavelength. The flow quantities of interest are discussed by graphical illustrations.

Key words: Jeffrey fluid, induced magnetic field, slip, heat and mass transfer.

INTRODUCTION

The study of peristaltic flow is of special interest for several applications in industry and physiology. Especially the peristaltic transport of non-Newtonian fluids (Ellahi, 2009) is a topic of major interest of the researchers in the physiological world. Such interest is stimulated because of its occurrence in several physiological processes including chyme movement in the gastrointestinal tract, urine transport from kidney to bladder, movement of ovum in the female fallopian tube, transport of spermatozoa in the ductus efferentes of the male reproductive tract, transport of bile in bile duct, in roller and finger pumps, in vasomotion of small blood vessels and many others. It is now a well accepted fact that the peristaltic flows of magnetohydrodynamic (MHD) fluids are important in medical sciences and bioengineering. The MHD characteristics are useful in the development of magnetic devices, cancer tumor treatment, hyperthermia and blood reduction during surgeries. Hence several scientists having in mind such importance extensively discussed the peristalsis with magnetic field effects (Reddy and Raju, 2010; Tripathi, 2011; Hayat et al., 2011a; Abd elmaboud and Mekheimer, 2011; Hayat et al., 2010a). Further, Singh and Rathee (2010, 2011) discussed the blood flow in the presence of an applied magnetic field. The pulsatile blood flow in the presence of applied magnetic field and body acceleration is examined by Sanyal et al. (2007). It is noticed that although ample literature on MHD peristaltic flow in the presence of applied magnetic field is available, very little attention is paid to the influence of induced magnetic field in peristalsis (Hayat et al., 2008a, b; Hayat et al., 2011b; Kotkandapani and Srinivas, 2008; Ali et al., 2008). In continuation, the induced magnetic field effect on the peristaltic motion in couple stress and micropolar fluids is addressed by Mekheimer (2008a, b). Hayat et al. (2010b, c) extended such discussion to third order and Carreau fluids. Abd elamboud (2011) examined induced magnetic field effect on peristaltic flow in an annulus.

The goal of the present study is to discuss the effect of induced magnetic field on peristaltic flow of Jeffrey fluid in non-uniform channel. The heat transfer and slip effects are also considered. The heat transfer analysis in such

*Corresponding author. E-mail: pensy_t@yahoo.com. Tel: +92-51-90642172.

flow is important because of hemodialysis and oxygenation process. Further, there is always small amount of slippage in the real systems. Two different types of fluids exhibit slip effect. One case consists of fluids with very elastic properties and other rarefied gases. The slip effect appears in concentrated polymer solutions, molten polymers and non-Newtonian fluids. In the flow of dilute suspensions of particle, a clear layer is noticed next to a wall. Poiseuille observed such a layer using a microscope in the flow of blood through capillary vessels (Coleman et al., 1966). Few very recent contributions dealing with peristaltic flows subject to slip and heat transfer effects may be mentioned in the researches (Hayat et al., 2010d; Srinivas et al., 2009; Nadeem and Akram, 2010; Akbar et al., 2011).

ANALYSIS

We consider the MHD peristaltic flow of an incompressible Jeffrey fluid in a symmetric but non-uniform channel. The fluid is electrically conducting in the presence of constant magnetic field with strength H_0 applied normal to the flow. This gives rise to an induced magnetic field $\mathrm{H}'(\mathrm{h}'_{X'}(X',Y',t'),\mathrm{h}'_{Y'}(X',Y',t'),0)$ and ultimately the total magnetic field is $\mathrm{H}'^{+}(\mathrm{h}'_{X'}(X',Y',t'),\mathrm{H}'_0+\mathrm{h}'_{Y'}(X',Y',t'),0)$. The flow generation is possible because of travelling wave on the channel walls.

The relevant equations for the present flow problem are given by:

$$\nabla.\mathbf{H}'=0,\quad \nabla.\boldsymbol{\epsilon}'=0,\quad \nabla\times\boldsymbol{\epsilon}'=-\mu_e\frac{\partial\mathbf{H}'}{\partial t'},\qquad (1)$$

$$\nabla\times\mathbf{H}'=\mathbf{J}',\quad \mathbf{J}'=\boldsymbol{\sigma}\{\boldsymbol{\epsilon}'+\mu_e(\mathbf{V}'\times\mathbf{H}'^{+})\},\qquad (2)$$

$$\nabla.\bar{\boldsymbol{V}}'=0,\qquad (3)$$

$$\rho\left[\frac{\partial}{\partial t}+(\boldsymbol{V}'.\nabla)\right]\bar{\boldsymbol{V}}'=div\boldsymbol{T}-\mu_e\left\{(\mathbf{H}'^{+}.\nabla)-\frac{1}{2}(\mathbf{H}'^{+})^2\nabla\right\},\qquad (4)$$

$$\rho C_p\frac{dT'}{dt'}=\kappa\nabla^2T'+\boldsymbol{T}.\boldsymbol{L},\qquad (5)$$

with $L=grad\boldsymbol{V}'$ and Cauchy stress tensor $(\mathbf{T})$ and extra stress tensor $(\mathbf{S}')$ in Jeffrey fluid are

$$T=-p'\bar{I}+\mathbf{S}',\qquad (6)$$

$$\mathbf{S}'=\frac{\mu}{1+\lambda_1}(\dot{\gamma}+\lambda_2\ddot{\gamma}).\qquad (7)$$

In the aforementioned expressions, p' denotes the pressure, $\mathbf{J}$ the current density, $\boldsymbol{I}$ the identity tensor, μ_e the magnetic permeability, ρ the fluid density, $\boldsymbol{\sigma}$ the electrical conductivity, $\boldsymbol{\epsilon}'$ an induced magnetic field, C_p the specific heat at a constant volume, κ the thermal conductivity, T the temperature, μ the dynamic viscosity of fluid, γ the shear rate, λ_1 the ratio of relaxation to retardation times, and λ_2 the retardation time and dots characterize material differentiation.

Induction equation in view of combination of Equations (1) and (2) becomes

$$\frac{\partial\mathbf{H}^{+}}{\partial t}=\nabla\times(\boldsymbol{V}\times\mathbf{H}^{+})+\frac{1}{\xi}\nabla^2\mathbf{H}^{+},\qquad (8)$$

where $\xi=1/\mu\boldsymbol{\sigma}$ is the magnetic diffusivity.

We perform the flow analysis in wave frame (x',y'). Hence the coordinates and velocities in the laboratory (X',Y') and wave (x',y') frames can be related through the following transformations:

$$x'=X'-ct',\ y'=Y',u'(x',y')=U'-c,v'(x',y')=V'\qquad (9)$$

where (U',V') and (u',v') are the respective velocities in the laboratory and wave frames.

The velocity V is chosen as follows:

$$\bar{V}'=(u',v',0).\qquad (10)$$

Introducing the non-dimensional quantities

$$x=\frac{x'}{\lambda},\ y=\frac{y'}{a},\ u=\frac{u'}{c},\ v=\frac{v'}{c},\ t=\frac{t'c}{\lambda},\ p=\frac{a^2p'}{c\lambda\mu},\ S=\frac{aS'}{\mu c},$$

$$h=\frac{h'}{a},\ \Psi=\frac{\Psi'}{ca},\ \Phi=\frac{\Phi'}{H_0a},\ \delta=\frac{\lambda}{a},\ R_e=\frac{\rho ca}{\mu},\ R_e=\sigma\mu_e ac,$$

$$S_1=\frac{H_0}{c}\sqrt{\frac{\mu_e}{\rho}},\ p_m=p+\frac{1}{2}R_e\delta\frac{\mu_e(\mathrm{H}^{+})^2}{\rho c^2},\ Br=E_rP_r,\ \theta'=\frac{T-T_0}{T_1-T_0},$$

$$P_r=\frac{\rho\nu C_p}{\kappa},\ E_r=\frac{c^2}{C_p(T_1-T_0)},\ Sc=\frac{\mu}{\rho D},\ Sr=\frac{\rho T_0DK_T}{\mu T_mC_0},\qquad (11)$$

$$u=\frac{\partial\Psi}{\partial y},\quad v=-\delta\frac{\partial\Psi}{\partial x},\quad h_x=\frac{\partial\Phi}{\partial y},\quad h_y=-\delta\frac{\partial\Phi}{\partial x},\qquad (12)$$

the incompressibility condition is satisfied whereas the other equations give

$$R_e\delta\left(\frac{\partial\Psi}{\partial y}\frac{\partial^2\Psi}{\partial x\partial y}-\frac{\partial\Psi}{\partial x}\frac{\partial^2\Psi}{\partial y^2}\right)=-\frac{\partial p_m}{\partial x}+\delta\frac{\partial}{\partial x}(S_{xx})+\frac{\partial}{\partial y}(S_{xy})+R_eS_1^2\frac{\partial^2\Phi}{\partial y^2}+R_eS_1^2\delta\left(\frac{\partial\Phi}{\partial y}\frac{\partial^2\Phi}{\partial x\partial y}-\frac{\partial\Phi}{\partial x}\frac{\partial^2\Phi}{\partial y^2}\right),\qquad (13)$$

$$R_e\delta^3\left(\frac{\partial\Psi}{\partial x}\frac{\partial^2\Psi}{\partial x\partial y}-\frac{\partial\Psi}{\partial y}\frac{\partial^2\Psi}{\partial x^2}\right)=$$
$$-\frac{\partial p_m}{\partial y}+\delta^2\frac{\partial}{\partial x}\left(S_{yx}\right)+\delta\frac{\partial}{\partial y}\left(S_{yy}\right)-R_e\delta^2S_1^2\frac{\partial^2\Phi}{\partial x\partial y}-R_eS_1^2\delta^3\left(\frac{\partial\Phi}{\partial y}\frac{\partial^2\Phi}{\partial x^2}-\frac{\partial\Phi}{\partial x}\frac{\partial^2\Phi}{\partial x\partial y}\right), \tag{14}$$

$$\frac{\partial\Psi}{\partial y}-\delta\left(\frac{\partial\Psi}{\partial y}\frac{\partial\Phi}{\partial x}-\frac{\partial\Psi}{\partial x}\frac{\partial\Phi}{\partial y}\right)+\frac{1}{R_m}\left(\frac{\partial^2\Phi}{\partial y^2}+\delta^2\frac{\partial^2\Phi}{\partial x^2}\right)=E, \tag{15}$$

$$R_e\delta\left(\frac{\partial\Psi}{\partial y}\frac{\partial\theta'}{\partial x}-\frac{\partial\Psi}{\partial x}\frac{\partial\theta'}{\partial y}\right)=\frac{1}{P_r}\left(\delta^2\frac{\partial^2\theta'}{\partial x^2}+\frac{\partial^2\theta'}{\partial y^2}\right)+E_r\left\{\begin{array}{c}\delta S_{xx}\frac{\partial^2\Psi}{\partial x\partial y}+S_{xy}\\ \left(\frac{\partial^2\Psi}{\partial y^2}-\delta^2\frac{\partial^2\Psi}{\partial x^2}\right)-\delta S_{yy}\frac{\partial^2\Psi}{\partial y\partial x}\end{array}\right\}, \tag{16}$$

$$R_e\delta\left(\frac{\partial\Psi}{\partial y}\frac{\partial\varphi}{\partial x}-\frac{\partial\Psi}{\partial x}\frac{\partial\varphi}{\partial y}\right)=\frac{1}{Sc}\left(\delta^2\frac{\partial^2\varphi}{\partial x^2}+\frac{\partial^2\varphi}{\partial y^2}\right)+Sr\left(\delta^2\frac{\partial^2\theta'}{\partial x^2}+\frac{\partial^2\theta'}{\partial y^2}\right), \tag{17}$$

where Ψ, Φ, E_r, P_r, Sc, Sr, δ, R_e, R_m, and S_1 are respectively the stream function, magnetic force function, Eckert, Prandtl, Schmidt, Soret, wave, Reynolds, magnetic Reynolds and Strommer's numbers. Here p_m shows the total pressure which is sum of ordinary and magnetic pressures. Further, T_0, C_0 and T_1, C_1 are the temperatures and concentrations at the upper and lower walls respectively and

$$S_{xx}=\frac{2\delta}{1+\lambda_1}\left(1+\frac{\lambda_2c\delta}{d_1}\left(\frac{\partial\Psi}{\partial y}\frac{\partial}{\partial x}-\frac{\partial\Psi}{\partial x}\frac{\partial}{\partial y}\right)\right)\frac{\partial^2\Psi}{\partial x\partial y},$$

$$S_{xy}=\frac{1}{1+\lambda_1}\left(1+\frac{\lambda_2c\delta}{d_1}\left(\frac{\partial\Psi}{\partial y}\frac{\partial}{\partial x}-\frac{\partial\Psi}{\partial x}\frac{\partial}{\partial y}\right)\right)\left(\frac{\partial^2\Psi}{\partial y^2}-\delta^2\frac{\partial^2\Psi}{\partial x^2}\right),$$

$$S_{yy}=-\frac{2\delta}{1+\lambda_1}\left(1+\frac{\lambda_2c\delta}{d_1}\left(\frac{\partial\Psi}{\partial y}\frac{\partial}{\partial x}-\frac{\partial\Psi}{\partial x}\frac{\partial}{\partial y}\right)\right)\frac{\partial^2\Psi}{\partial x\partial y},$$

with the boundary conditions given following

$$\Psi=0,\ \ \frac{\partial^2\Psi}{\partial y^2}=0,\ \ \frac{\partial\Phi}{\partial y}=0,\ \ \frac{\partial\theta'}{\partial y}=0,\ \ \frac{\partial\varphi}{\partial y}=0,\ \ at\ \ y=0, \tag{18}$$

$$\Psi=F,\ \ \frac{\partial\Psi}{\partial y}=-\beta S_{xy}-1,\ \ \Phi=1,\ \ \theta'=1,\ \ \varphi=0,\ \ at\ \ y=h(x), \tag{19}$$

where the dimensionless slip parameter $\beta(=L/a)$.

In view of long wavelength and low Reynolds number analysis, one has from Equations (13) to (19) as

$$-\frac{\partial p}{\partial x}+\frac{\partial}{\partial y}\left(\frac{1}{1+\lambda_1}\frac{\partial^2\Psi}{\partial y^2}\right)+R_eS_1^2\frac{\partial^2\Phi}{\partial y^2}=0, \tag{20}$$

$$-\frac{\partial p}{\partial y}=0, \tag{21}$$

$$\frac{\partial^2\Phi}{\partial y^2}=R_m\left(E-\frac{\partial\Psi}{\partial y}\right). \tag{22}$$

Equations (21) and (22) after eliminating the pressure give

$$\frac{\partial^2}{\partial y^2}\left(\frac{1}{1+\lambda_1}\frac{\partial^2\Psi}{\partial y^2}\right)+R_eS_1^2\frac{\partial^3\Phi}{\partial y^3}=0. \tag{23}$$

Now Equations (17) and (18) are presented in the forms

$$\frac{\partial^2\theta'}{\partial y^2}+Br\left\{\frac{1}{1+\lambda_1}\left(\frac{\partial^2\Psi}{\partial y^2}\right)^2\right\}=0, \tag{24}$$

$$\frac{1}{Sc}\frac{\partial^2\varphi}{\partial y^2}+Sr\frac{\partial^2\theta'}{\partial y^2}=0, \tag{25}$$

with the boundary conditions as follows

$$\Psi=0,\ \ \frac{\partial^2\Psi}{\partial y^2}=0,\ \ \frac{\partial\Phi}{\partial y}=0,\ \ \frac{\partial\theta'}{\partial y}=0,\ \ \frac{\partial\varphi}{\partial y}=0,\ \ at\ \ y=0, \tag{26}$$

$$\Psi=F,\ \ \frac{\partial\Psi}{\partial y}=-\frac{\beta}{1+\lambda_1}\frac{\partial^2\Psi}{\partial y^2}-1,\ \ \Phi=1,\ \ \theta'=1,\ \ \varphi=0,\ \ at\ \ y=h(x). \tag{27}$$

Our interest in this study is to perform the analysis for the following wave forms.

(1) Sinusoidal wave $h(x)=1+Kx+\phi\sin\left(2\pi(x-t)\right)$.

(2) Triangular wave

$$h(x)=1+Kx+\phi\left[\frac{8}{\pi^3}\sum_{m=1}^{\infty}\frac{(-1)^{m+1}}{(2m-1)^2}\sin\{2(2m-1)\pi(x-t)\}\right].$$

(3) Square wave

$$h(x)=1+Kx+\phi\left[\frac{4}{\pi}\sum_{m=1}^{\infty}\frac{(-1)^{m+1}}{(2m-1)}\cos\{2(2m-1)\pi(x-t)\}\right].$$

(4) Trapezoidal wave

$$h(x)=1+Kx+\phi\left[\frac{32}{\pi^2}\sum_{m=1}^{\infty}\frac{(-1)^{m+1}\sin\left\{\frac{\pi}{8}(2m-1)\right\}}{(2m-1)^2}\sin\{2(2m-1)\pi(x-t)\}\right],$$

with $\phi=b/a$ (amplitude ratio) and $K=\lambda k/a(k\ll 1)$. Total number of terms in the series that are incorporated in the analysis are 50. Note that the expressions for triangular, square and trapezoidal waves are derived from Fourier series.

The pressure rise per wavelength is

$$\Delta p_\lambda=\int_0^1\frac{dp}{dx}dx. \tag{28}$$

EXACT SOLUTION

From Equations (20), (22) and (23) we have

$$\frac{\partial p}{\partial x} = \frac{\partial}{\partial y}\left(\frac{1}{1+\lambda_1}\frac{\partial^2 \Psi}{\partial y^2}\right) + M^2\left(E - \frac{\partial \Psi}{\partial y}\right), \tag{29}$$

$$\frac{\partial^4 \Psi}{\partial y^4} - (1+\lambda_1)M^2\frac{\partial^2 \Psi}{\partial y^2} = 0. \tag{30}$$

The aforementioned equations along with the corresponding boundary conditions give

$$\Psi = \frac{1}{L^2}\{(\cosh(Ly) - \sinh(Ly))(C_2 + C_1\cosh(2Ly) + C_1\sinh(2Ly))\} + C_3 + C_4 y, \tag{31}$$

$$\frac{dp}{dx} = \frac{(C_1 - C_2)L}{(1+\lambda_1)} - \frac{\{(C_1 - C_2)L + L^2(C_4 - E)\}}{L}, \tag{32}$$

$$C_1 = -\frac{(F+h)(1+\lambda_1)L^2}{2L_1}, \quad C_2 = \frac{(F+h)(1+\lambda_1)L^2}{2L_1}, \quad C_3 = 0,$$

$$C_4 = \frac{FL(1+\lambda_1)\cosh(hL) + (1+F\beta L^2 + \lambda_1)\sinh(hL)}{L_1},$$

where $M^2 = R_m R_e S_1^2$ (is the Hartman number), $L = M\sqrt{(1+\lambda_1)}$;
$L_1 = hL(1+\lambda_1)\cosh(hL) + (-1 + hL^2\beta - \lambda_1)\sinh(hL)$.
The corresponding systems for Φ and θ after using Equation (31) finally give

$$\Phi = \frac{1}{2LM^2(1+\lambda_1)}\left(2L^3(C_5 - C_6 y) - \left(L^3y^2(C_4 - E) + 2(C_1 - C_2)\cosh(Ly) + 2(C_1 + C_2)\sinh(Ly)\right)R_m\right), \tag{33}$$

$$\theta' = -\frac{1}{4L^4}\left(-4\left(-BrC_1C_2L^4y^2 + L^4(C_7 \mp y)\right) + Br(C_1^2 + C_2^2)L^2\cosh(2Ly) + Br(C_1^2 - C_2^2)L^2\sinh(2Ly)\right), \tag{34}$$

$$C_5 = \frac{(hL(2(C_1+C_2) + hL^2(C_4 - E) + 2(C_1 - C_2)\cosh(hL) + 2(C_1+C_2)\sinh(hL))R_m}{2L^3},$$

$$C_6 = \frac{(C_1 + C_2)R_m}{L^2}, \quad C_8 = \frac{Br(C_1^2 - C_2^2)}{2L},$$

$$C_7 = \frac{Br(2hL(-C_1^2 + C_2^2 + 2C_1C_2hL) + (C_1^2 + C_2^2)\cosh(2hL) - (C_1^2 - C_2^2)\sinh(2hL))}{4L^2}.$$

Now the results for axial induced magnetic field h_x, current density distribution J_z and concentration distribution φ are given by

$$h_x = \frac{C_6L^2 - (L^2y + (C_1 + C_2)\cosh(Ly) + 2(C_1 - C_2)\sinh(Ly))R_m}{L^2}, \tag{35}$$

$$J_z = \frac{(2L^3(C_4 - E) + 2(C_1 - C_2)L^2\cosh(hL) + 2(C_1 + C_2)L^2\sinh(Ly))R_m}{2L^3}, \tag{36}$$

$$\varphi = \frac{1}{4L^4}\left(4\left(C_9L^4 + y(BrC_1C_2L^4yScSr + C_{10}L^4)\right) + Br(C_1^2 + C_2^2)ScSrL^2\cosh(2Ly) + Br(C_1^2 - C_2^2)ScSrL^2\sinh(2Ly)\right), \tag{37}$$

$$C_9 = \frac{BrL^2ScSr(2hL(-C_1^2 + C_2^2 + 2C_1C_2hL) + (C_1^2 + C_2^2)\cosh(2hL) + (C_1^2 - C_2^2)\sinh(2hL)}{2L^4},$$

$$C_{10} = \frac{Br(C_1^2 - C_2^2)ScSr}{2L},$$

RESULTS AND DISCUSSION

In order to predict the effects of pertinent parameters on various quantities such as pressure rise per wavelength (Δp_λ), the streamlines (Ψ), the axial induced magnetic field (h_x), the current density distribution (J_z), the temperature (θ') and concentration (φ) distributions, the Figures 1-7 are displayed for different wave forms. This analysis mainly focuses for the effects of slip parameter (β), Hartman number (M), the ratio of relaxation to retardation times (λ_1), Brinkman number (Br), Schmidt number (Sc) and Soret number (Sr).

Figures 1(a-d) characterize the pumping mechanism for different values of λ_1. There are four types of regions regarding pumping. When the dimensionless mean flow rate (θ) and pressure rise per wavelength (Δp_λ) are positive it defines the peristaltic pumping region. For $\theta > 0$ and $\Delta p_\lambda < 0$, we have augmented pumping and for $\theta = 0$, $\Delta p_\lambda > 0$ is a free pumping region. One also has retrograde pumping when $\theta > 0$ and $\Delta p_\lambda < 0$. Figure 1a shows clearly that for sinusoidal wave, the Δp_λ increases for small values of λ_1 in retrograde pumping region whereas a reverse situation is noticed in the augmented region, that is Δp_λ increases by increasing λ_1. The other wave forms also show the similar behavior as that of sinusoidal wave. It is also observed that Δp_λ is maximum for square wave and minimum for triangular wave. The variation of M on axial induced magnetic field (h_x) with y over a cross section $x = 0.1$ is displayed in the Figures 2(a-d). It is revealed from the Figure 2a that magnitude of axial induced magnetic field (h_x) increases for M. Interestingly, the axial induced magnetic field (h_x) in the upper half region is in one direction while

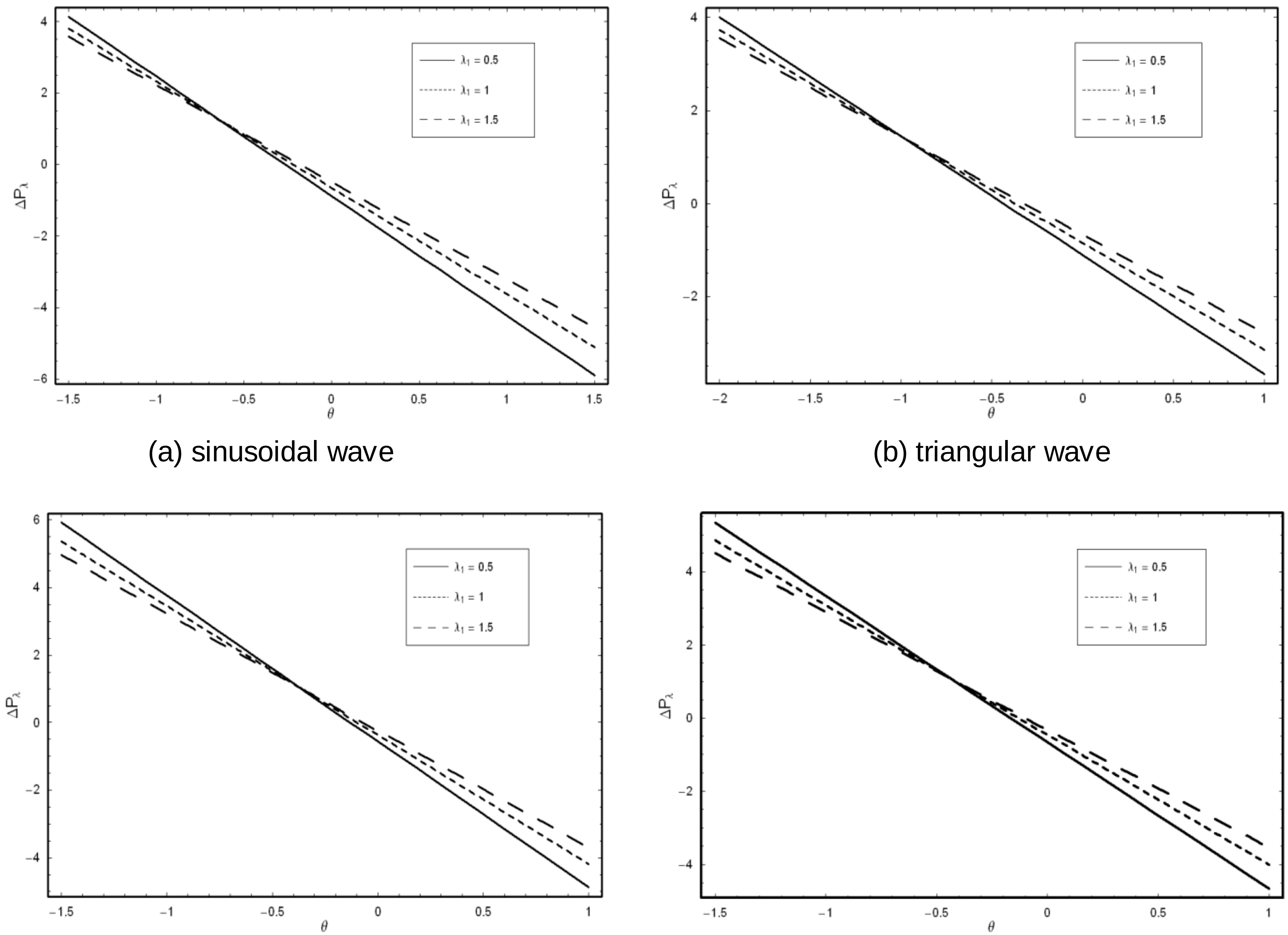

(a) sinusoidal wave

(b) triangular wave

(c) square wave

(d) trapezoidal wave

Figure 1. Plot for Δp_λ versus x. The other parameters are $K = 0.005,\ \phi = \frac{\pi}{6},\ E = 0.4,\ t = 0.1,\ \beta = 0.2,\ R_e = R_m = S_1 = M = 1.$

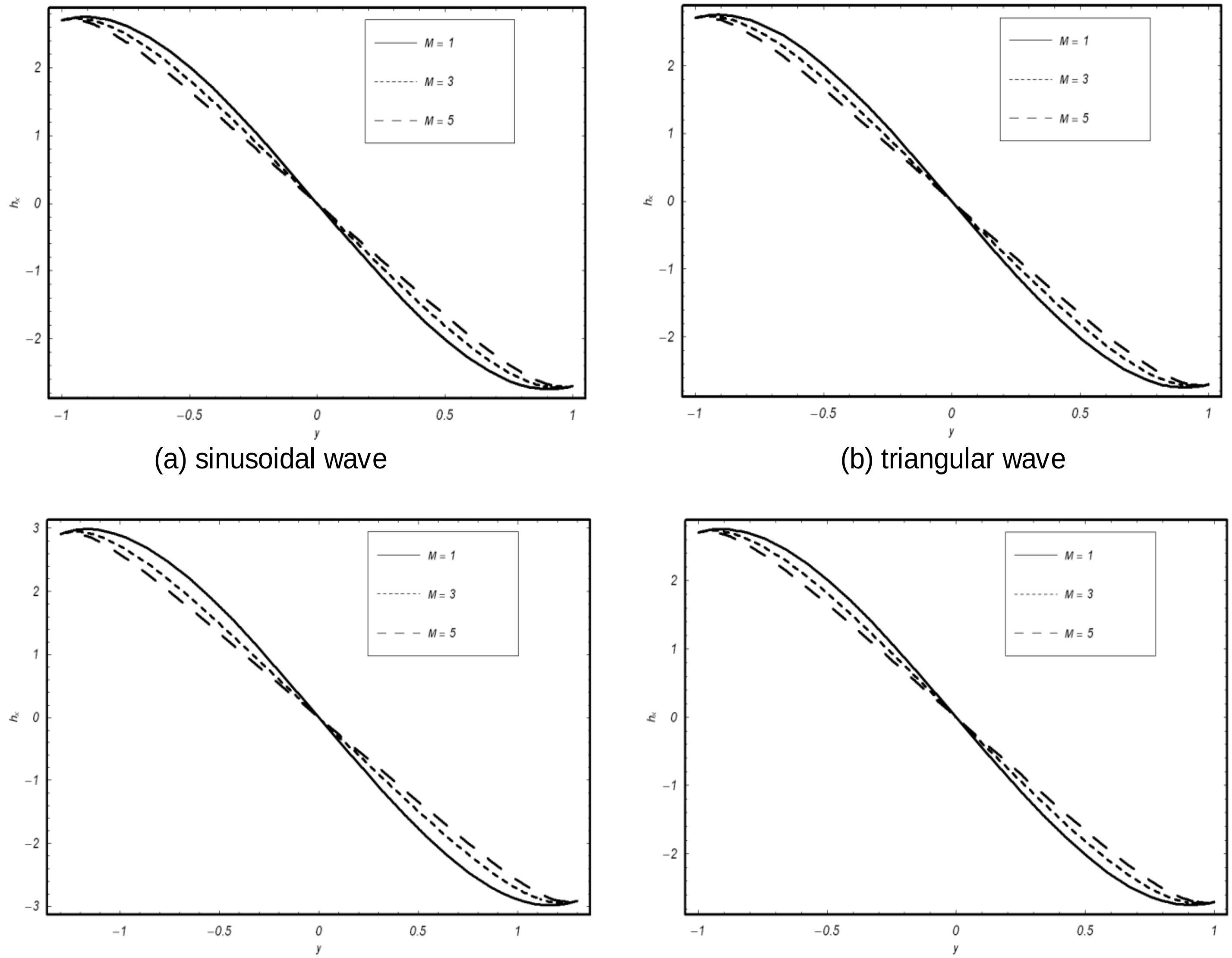

(a) sinusoidal wave (b) triangular wave

(c) square wave (d) trapezoidal wave

Figure 2. Variation of h_x versus y. Here $K = 0.005,\ \phi = \frac{\pi}{6},\ \mathrm{E} = 0.3,\ \mathrm{t} = 0.1,\ \beta = 0.03,\ \lambda_1 = 0.05,\ R_m = 1, \theta = 3$ and $\mathrm{x} = 0.1$.

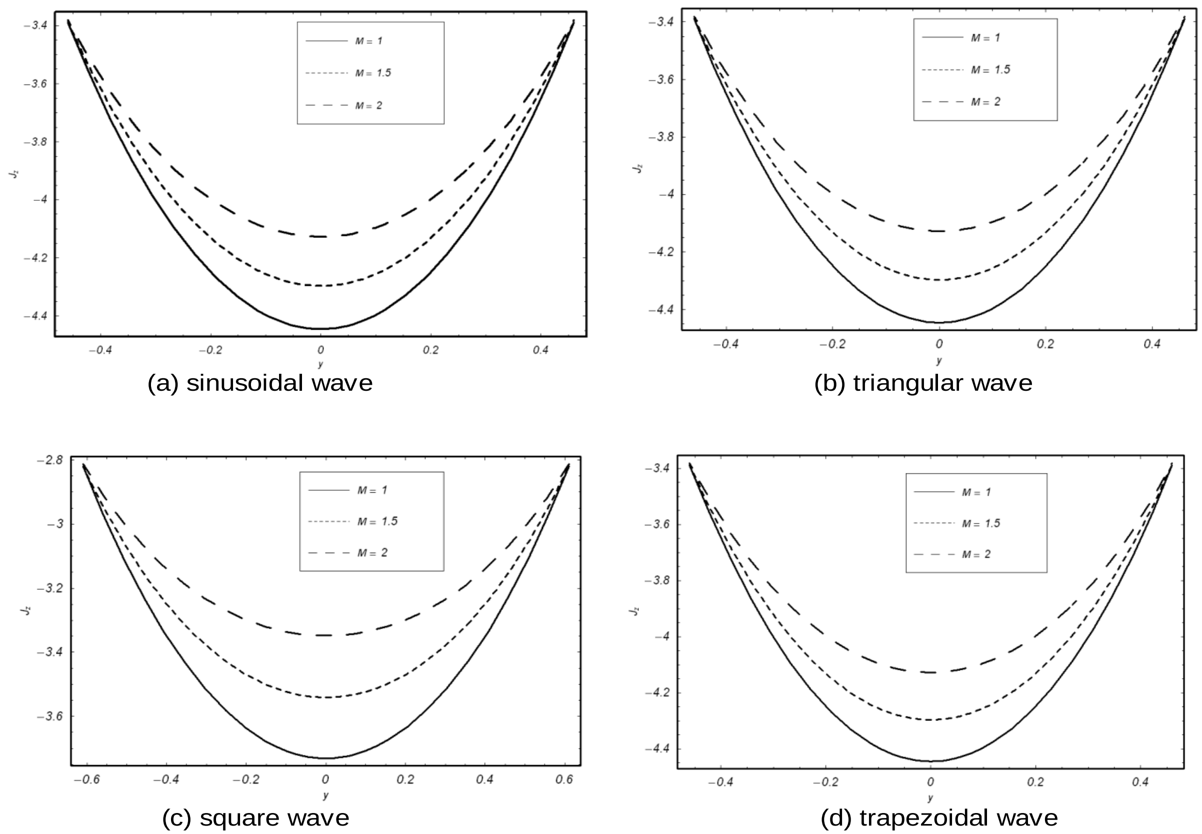

Figure 3. Variation of J_z versus y. Here $K = 0.005,\ \phi = \frac{\pi}{6},\ E = 0.3,\ t = 0.1,\ \beta = 0.03,\ \lambda_1 = 0.05,\ R_m = 1, \theta = 3$ and $x = 0.1$.

it is in the opposite direction in the lower half region. Further, h_x is equal to zero at $y = 0$. These results also hold for all the other considered wave forms in Figure 2(c-d). A comparative study further indicates that h_x is maximum for square wave and minimum for trapezoidal wave. To see the variation of current density distribution (J_z) versus y over a cross section $x = 0.1$, we have plotted the Figures 3(a-d). Here we found that J_z is an increasing function of M. Trapping is an interesting phenomenon in theory of peristaltic transport. The formation of an internally circulating bolus of the fluid by closed streamlines is called trapping and this trapped bolus is pushed ahead along the peristaltic wave with the speed of wave. Here Figures 4-5 have been

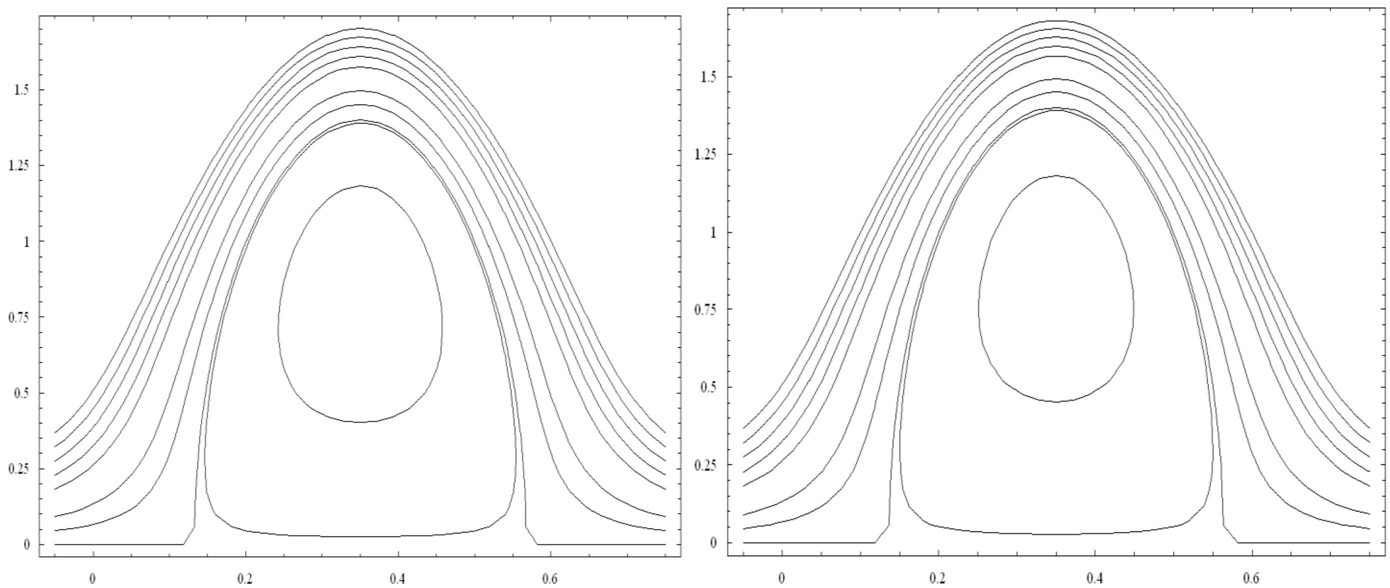

Figure 4a. Streamlines (sinusoidal wave) for $\lambda_1 = 0.5, \lambda_1 = 1.5$.

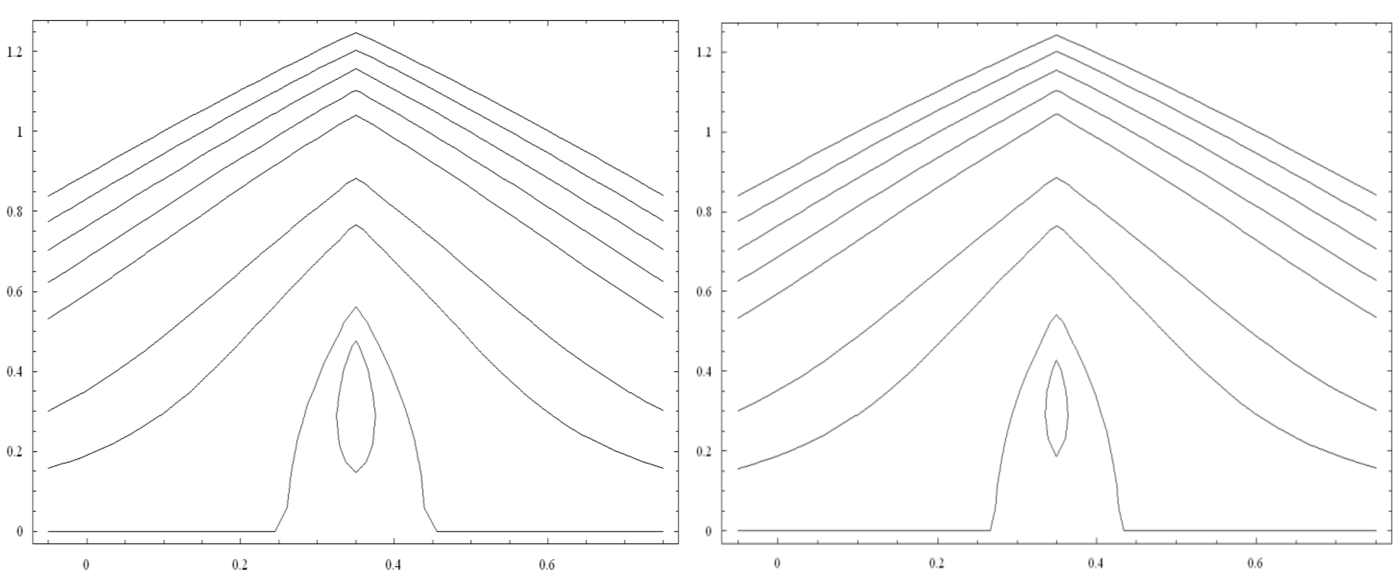

Figure 4b. Streamlines (triangular wave) for $\lambda_1 = 0.5, \lambda_1 = 1.5$.

plotted for the description of trapping when $M = 1, \beta = 0.03, \varphi = \frac{\pi}{6}, a = b = 0.4, d = 1.1$ and θ=0.61. The streamlines for different values of λ_1 are shown in Figure 4. It is noticed that the size of the trapped bolus decreases from $\lambda_1 = 0.5$ to $\lambda_1 = 1.5$. In Figure 5 we have sketched the streamlines for different values of M. This Figure depicts that trapping reduces for large values of M. That is size of the trapped bolus is going to squeeze from hydrodynamic to magneto-hydrodynamic situations for all the considered wave forms.

In the Figures 6(a-d) and 7(a-d), the temperature and concentration profiles have been illustrated. As expected, the temperature is an increasing function of Br (Figure 7). In fact Brinkman number is a measure of the importance of viscous heating relative to the conductive heat transfer.

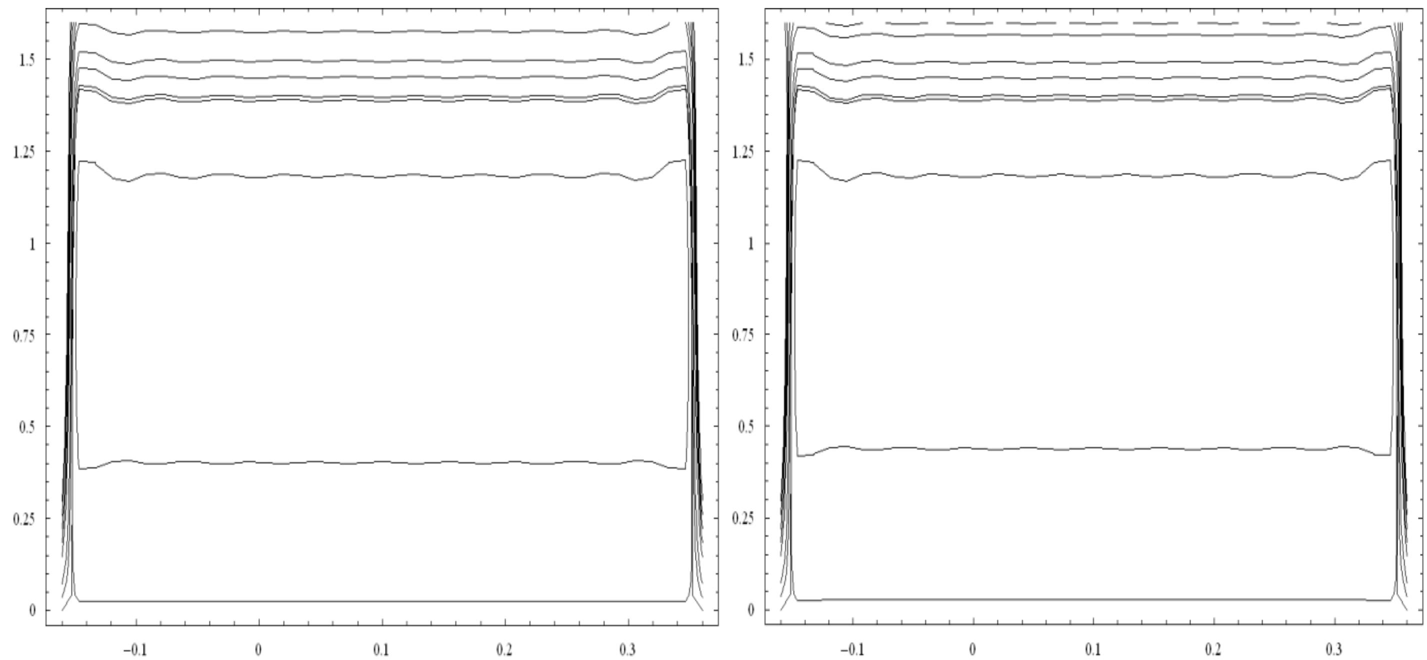

Figure 4c. Streamlines (square wave) for $\lambda_1 = 0.5, \lambda_1 = 1.5$.

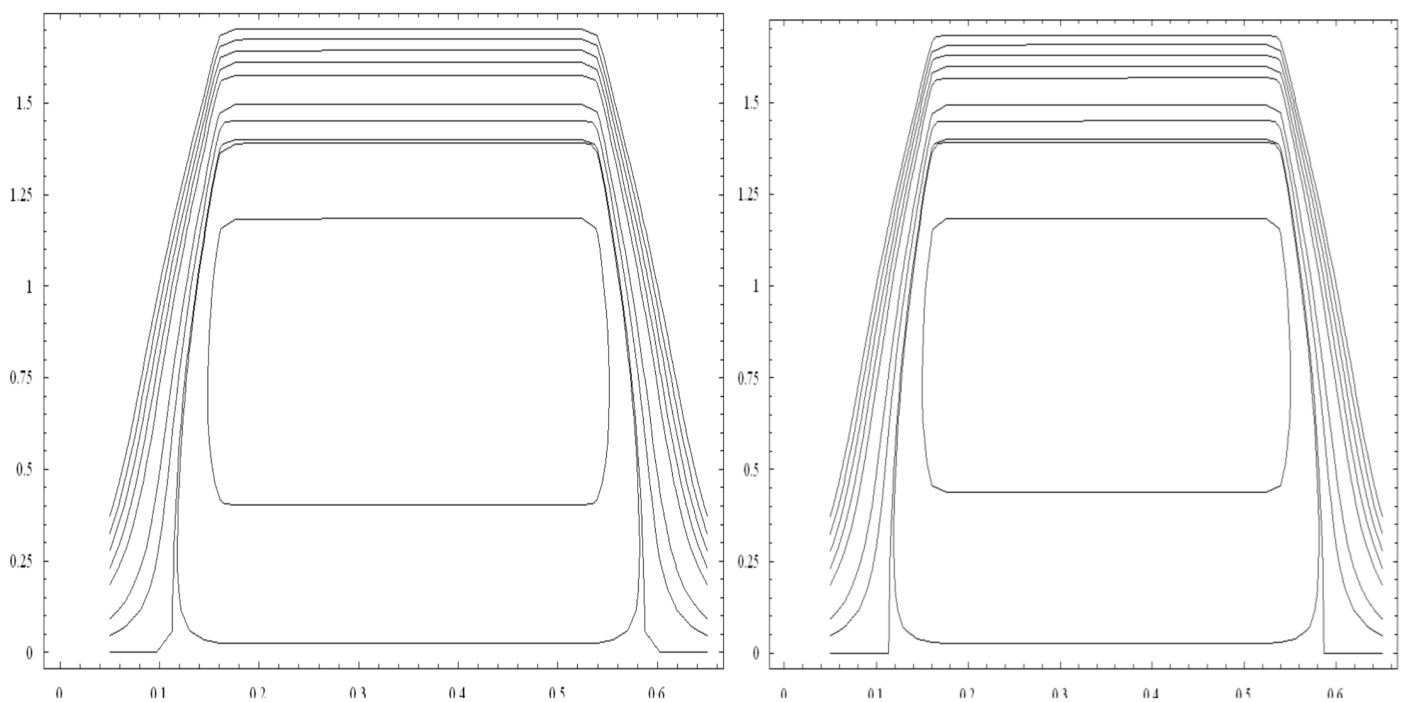

Figure 4d. Streamlines (trapezoidal wave) for $\lambda_1 = 0.5, \lambda_1 = 1.5$.

An increase in the Brinkman number increases the energy in the molecules and consequently the temperature increases. Here it is also observed that the temperature profile looks almost parabolic. The temperature is maximum for the sinusoidal and trapezoidal waves.

The Schmidt number is defined as the ratio of momentum diffusivity and mass diffusivity and is used to characterize the fluid flows in which there are simultaneous

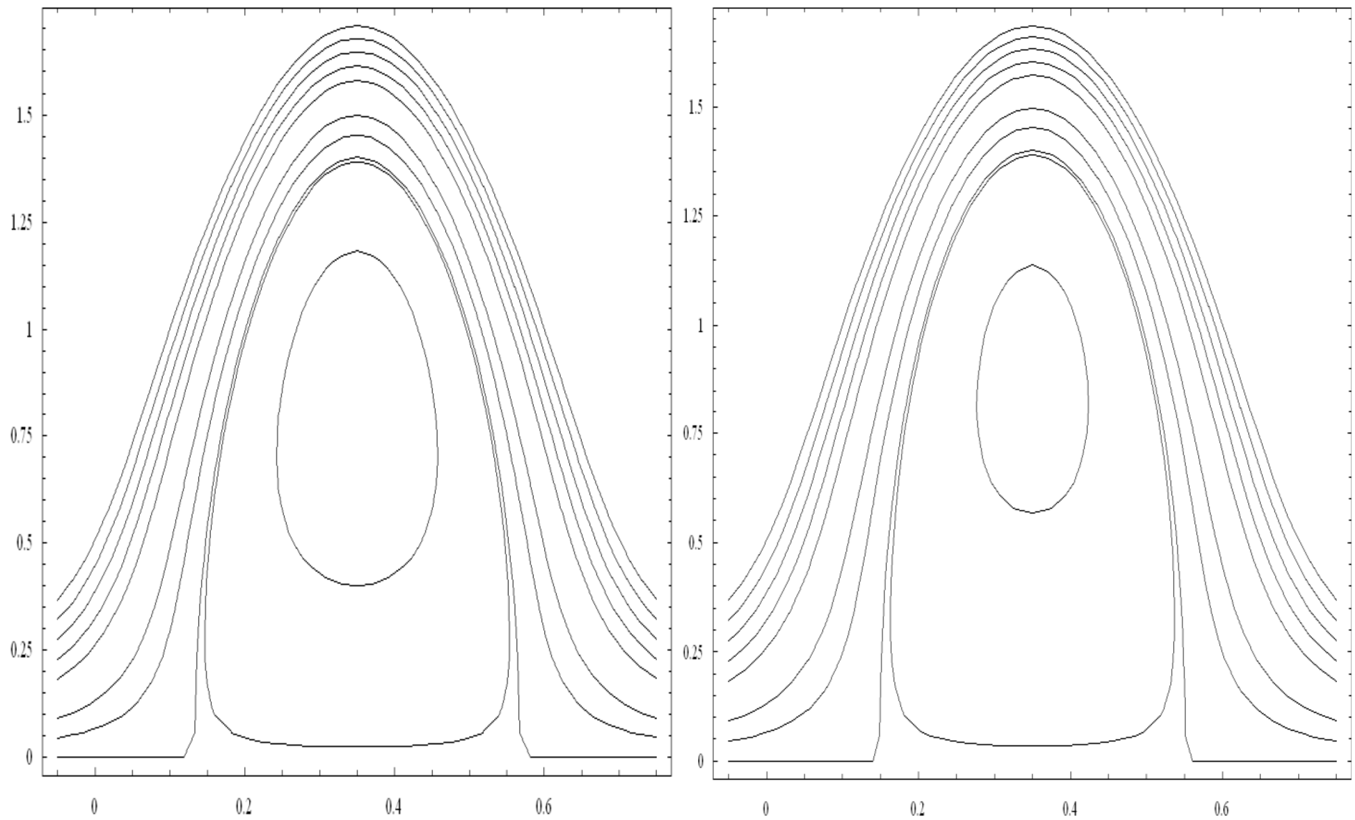

Figure 5a. Streamlines (sinusoidal wave) for $\mathrm{M} = 1, \mathrm{M} = 2$.

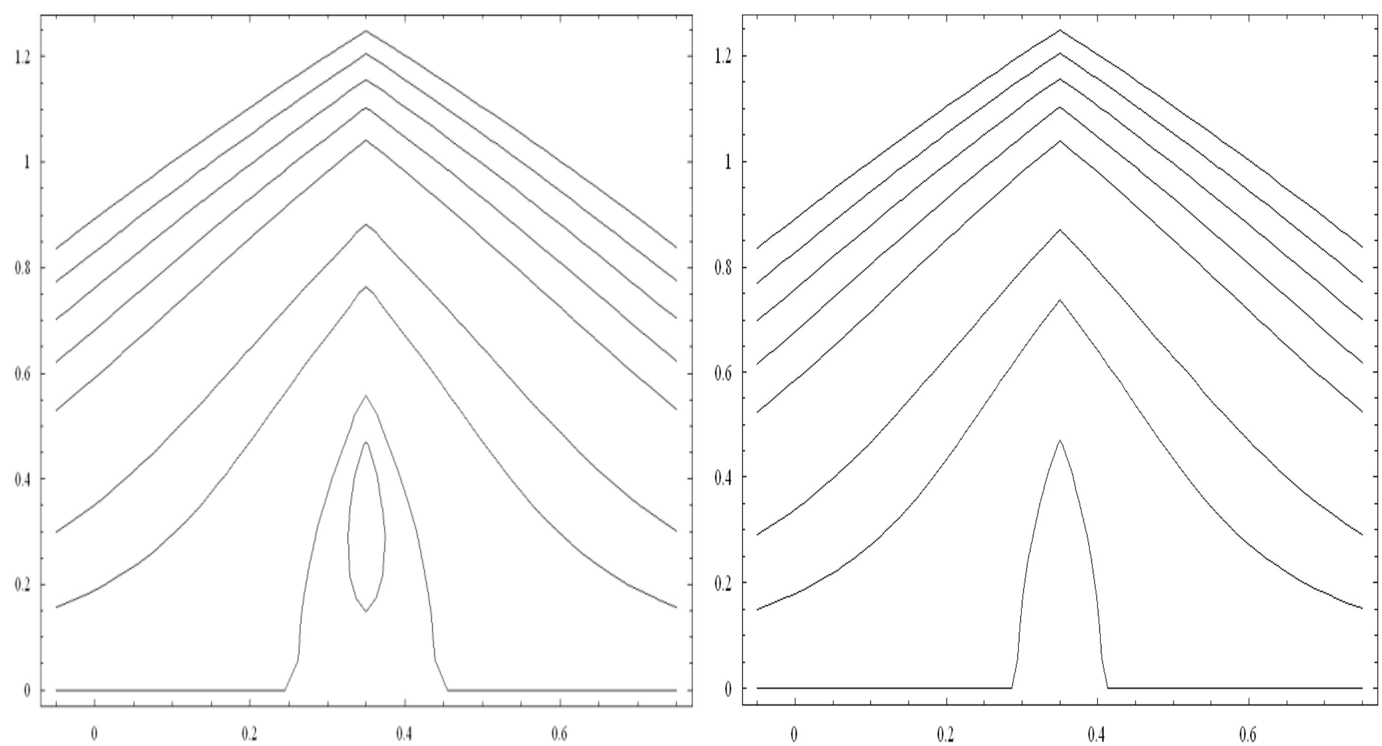

Figure 5b. Streamlines (triangular wave) for $\mathrm{M} = 1, \mathrm{M} = 2$.

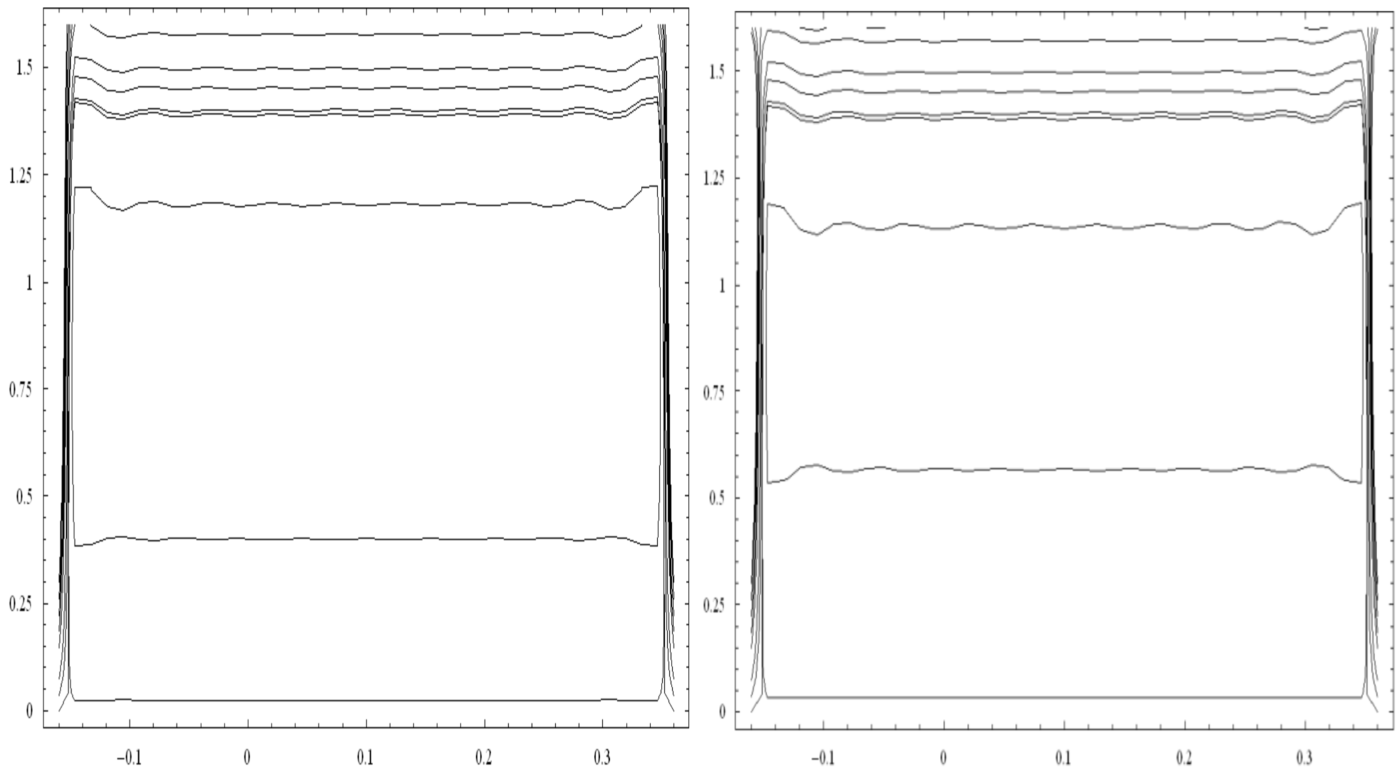

Figure 5c. Streamlines (square wave) for $M = 1, M = 2$.

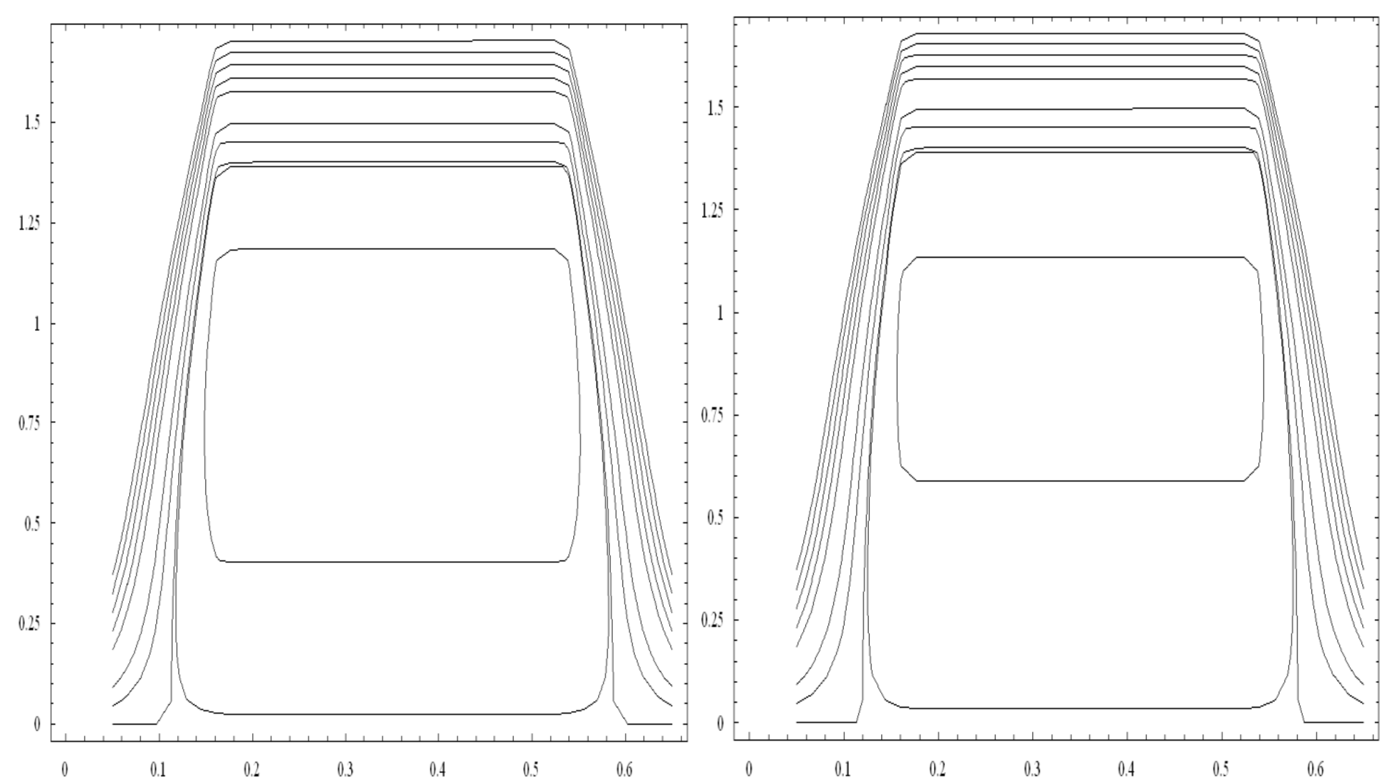

Figure 5d. Streamlines (trapezoidal wave) for $M = 1, M = 2$.

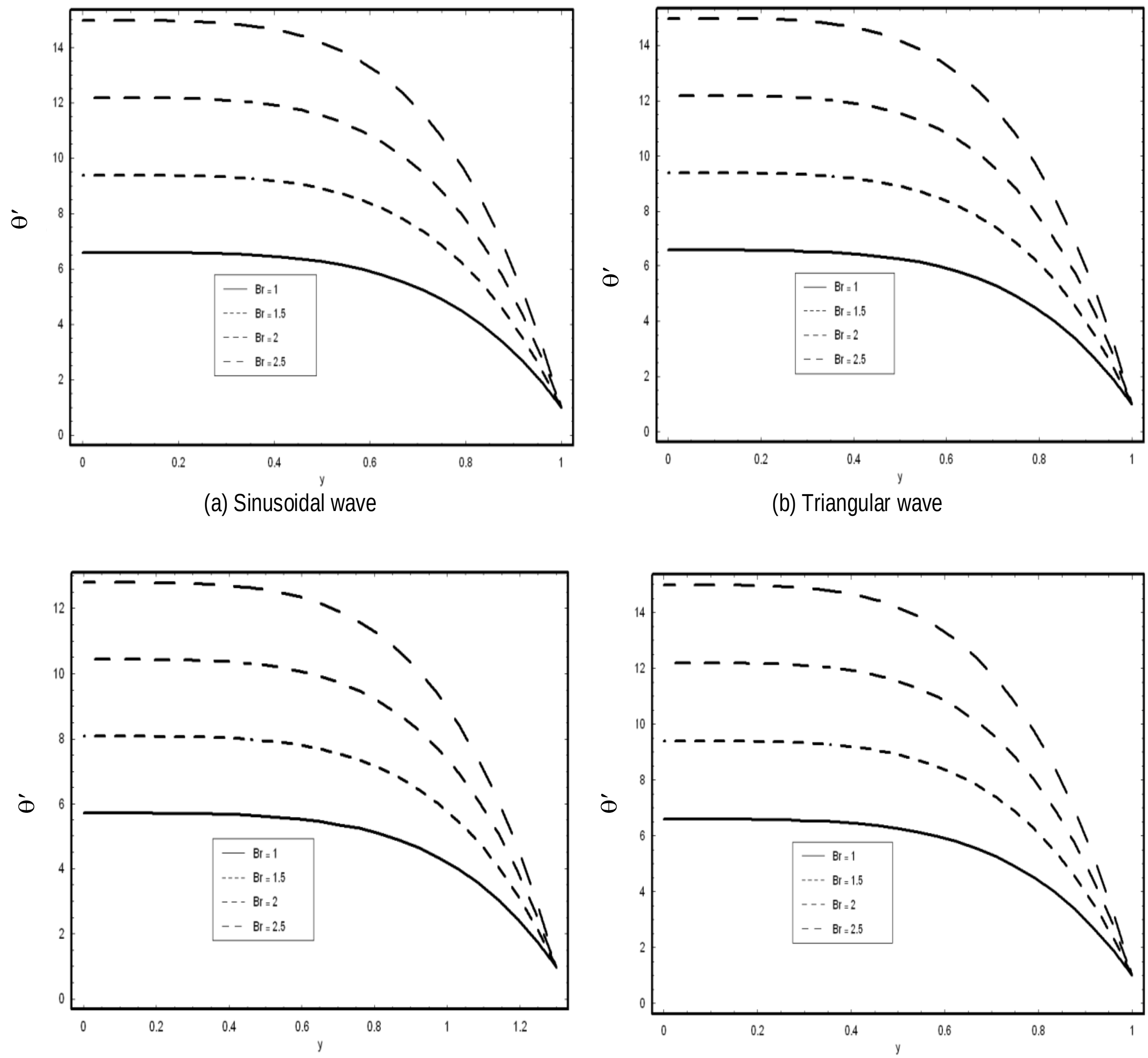

(a) Sinusoidal wave (b) Triangular wave (c) Square wave (d) Trapezoidal wave

Figure 6. Variation of θ' versus y. Here $K = 0.005,\ \phi = \frac{\pi}{6},\ E = 0.03,\ t = 0.1,\ \beta = 0.03,\ \lambda_1 = 0.4, M = 0.8,\ R_m = 1, a = b = 0.4, d = 1.1$ and $x = 0.1$

momentum and mass diffusion convection processes. Since Sc has a direct relation with mass diffusion rate therefore increases for small values of Sc. It is observed that such decrease is maximum for square wave form.

ACKNOWLEDGEMENT

The research of Ahmed Alsaedi was partially supported by Deanship of Scientific Research (DSR), King Abdulaziz University, Jeddah, Saudi Arabia.

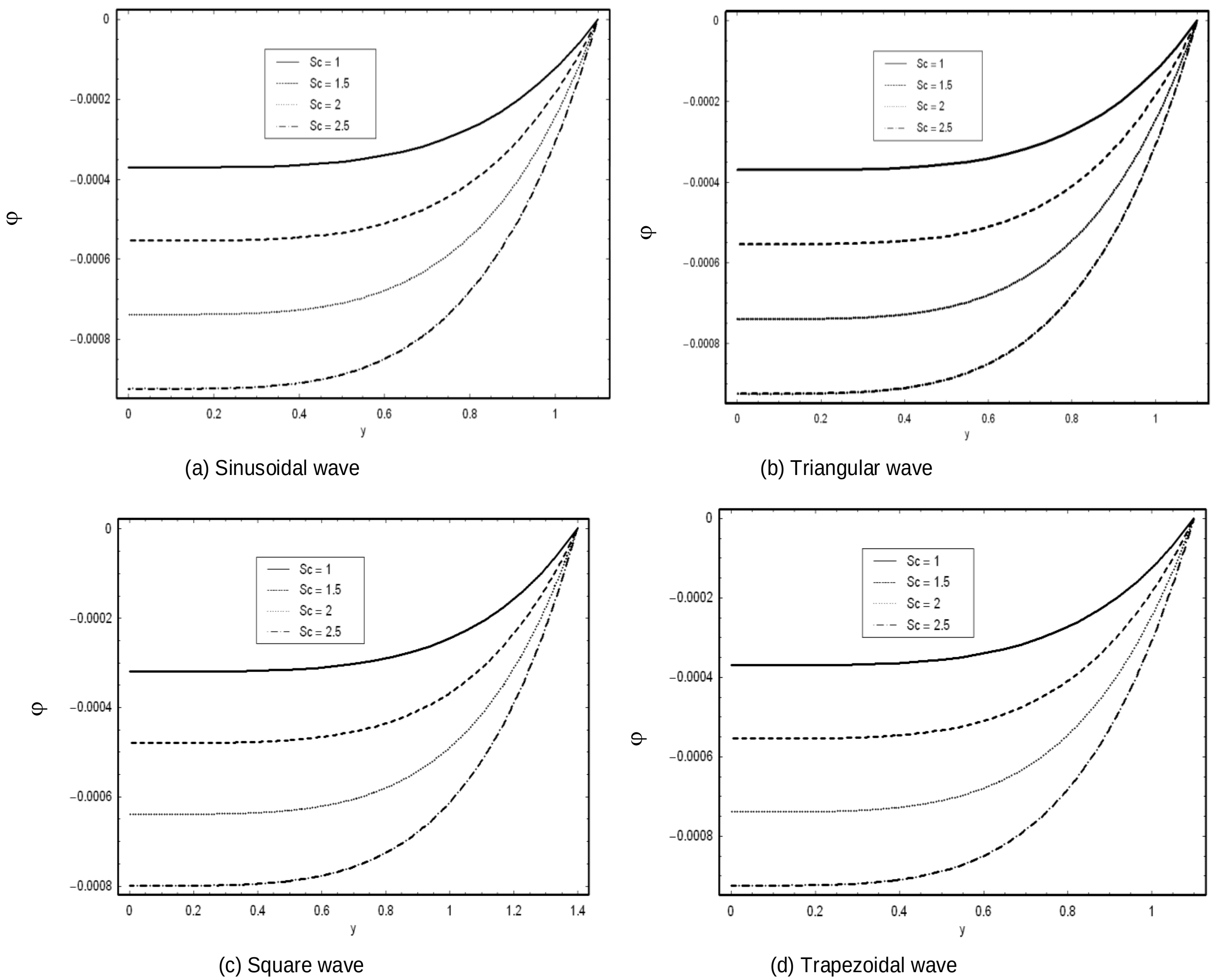

Figure 7. Variation of φ versus y. Here $K=0.005,\ \phi=\frac{\pi}{6},\ E=0.03,\ t=0.1,\ \beta=0.03,\ \lambda_1=0.4, M=0.8,\ R_m=1, \theta=2, Sc=Sr=1,\ a=b=0.4, d=1.1$ and $x=0.1$

REFERENCES

Abd elamboud Y, Mekheimer KhS (2011). Nonlinear peristaltic transport of a second order fluid through a porous medium. Appl. Math. Modelling, 35: 2695-2710.

Ali N, Hussain Q, Hayat T, Asghar S (2008). Slip effects on the peristaltic transport of MHD fluid with variable viscosity. Phys. Lett. A, 372: 1477-1489.

Abd elamboud Y (2011). Influence of induced magnetic field on peristaltic flow in an annulus. Comm. Nonlinear Sci. Numer. Simulation, in press.

Akbar NS, Hayat T, Nadeem S, Hendi AA (2011). Effects of slip and heat transfer on peristaltic flow of a third order fluid in an inclined asymmetric channel. Int. J. Heat and Mass Transfer, 54: 1654-1664.

Coleman BD, Markovitz H, Noll W (1966). Viscometric flows of non-Newtonian fluids. Springer- Verlag, Berlin, Heidelberg, New York.

Ellahi R (2009). Steady and unsteady flow for Newtonian and non-Newtonian fluids: Basics, concepts and methods. VDM, Germany.

Hayat T, Javid M, Hendi AA (2011a). Peristaltic transport of viscous fluid in a curved channel with compliant walls. Int. J. Heat Mass Transf., 54: 1615-1621.

Hayat T, Saleem N, Ali N (2010a). Peristaltic flow of a Carreau fluid in a channel with different wave forms. Numerical Methods for Partial Differential Equations, 26: 519-534

Hayat T, Hussain Q, Ali N (2008a). Influence of partial slip on the peristaltic flow in a porous medium. Physica A, 387: 3399-3409.

Hayat T, Qureshi MU, Ali N (2008b). The influence of slip on the peristaltic motion of a third order fluid in an asymmetric channel. Phys. Lett. A, 372:2653-2664.

Hayat T, Saleem N, Mesloub S, Ali N (2011b). MHD flow of a Carreau fluid in a channel with different wave forms, Zeitscrift fur Naturforschung A, 66a: 15-222.

Hayat T, Khan Y, Ali N, Mekheimer KhS (2010b). Effect of an induced magnetic field on the peristaltic flow of a third order fluid. Numerical

Methods for Partial Differential Equations, 26:345-366.
Hayat T, Saleem N and Ali N (2010c). Effect of induced magnetic field on peristaltic transport of a Carreau fluid, Commun. Nonlinear Sci. Numer. Simul., 15: 2407-2423.
Hayat T, Hina S, Ali N (2010d). Simultaneous effects of slip and heat transfer on peristaltic flow. Commun. Nonlinear Sci. Numer. Simul., 15: 1526-1537.
Kotkandapani M, Srinivas S (2008). Peristaltic transport of a Jeffrey fluid under the effect of magnetic field in an asymmetric channel. Int. J. Non-Linear Mech., 43: 915-924.
Mekheimer KhS (2008a). Effect of the induced magnetic field on peristaltic flow of a couple stress fluid. Phys. Lett. A, 372: 4271-4278.
Mekheimer KhS (2008b). Peristaltic flow of a magneto-micropolar fluid: Effect of induced magnetic field. J. Appl. Math., 2008: 1-23.
Nadeem S, Akaram S (2010). Heat transfer in peristaltic flow of MHD fluid with partial slip. Commun. Nonlinear Sci. Numer. Simul., 15: 312-321.
Reddy MS, Raju GSS (2010). Nonlinear peristaltic pumping of Johnson-Segalman fluid in an asymmetric channel under effect of a magnetic field. European J. Sci. Res., 46:147-164.
Sanyal DC, Das K, Debnath S (2007). Effect of magnetic field on pulsatile blood flow through an inclined circular tube with periodic body acceleration. Int. J. Phys. Sci. 11: 43-56.
Singh J, Rathee R (2010). Analytical solution of two-dimensional model of blood flow with variable viscosity through an indented artery due to LDL effect in the presence of magnetic field. Int. J. Phys. Sci., 5: 1857-1868.
Singh J, Rathee R (2011). Analysis of non-Newtonian blood flow through stenosed vessel in porous medium under the effect of magnetic field. Int. J. Phys. Sci., 6: 2497-2506.
Srinivas S, Gayathri R, Kothandapani M (2009). Influence of slip condition, wall properties and heat transfer on MHD peristaltic transport. Computer Physics Communications, 180: 2115-2122.
Tripathi D (2011). A mathematical model for the peristaltic flow of chyme movement in small intestine. Math. Biosciences, in press.

.